



HAL
open science

Sailing site investigation through CFD modelling of micrometeorology

Malo Le Guellec, Yann Amice

► **To cite this version:**

Malo Le Guellec, Yann Amice. Sailing site investigation through CFD modelling of micrometeorology. The Third International Conference on Innovation in High Performance Sailing Yachts, INNOVSAIL, Lorient, France, Jun 2013, Lorient, France. pp.223-228. hal-02110243

HAL Id: hal-02110243

<https://hal.science/hal-02110243>

Submitted on 25 Apr 2019

HAL is a multi-disciplinary open access archive for the deposit and dissemination of scientific research documents, whether they are published or not. The documents may come from teaching and research institutions in France or abroad, or from public or private research centers.

L'archive ouverte pluridisciplinaire **HAL**, est destinée au dépôt et à la diffusion de documents scientifiques de niveau recherche, publiés ou non, émanant des établissements d'enseignement et de recherche français ou étrangers, des laboratoires publics ou privés.

SAILING SITE INVESTIGATION THROUGH CFD MODELLING OF MICROMETEOROLOGY

M. Le Guellec, Fluidyn FRANCE, France, malo.leguellec@fluidyn.com

Y. Amice, Département Météorologie - Institut de Recherche de l'École Navale, France, yann.amice@gmail.com;

To have a prior accurate knowledge of the local wind currents on a water body is of crucial importance for the performance of the sailing team. In the recent years, Computational Fluid Dynamics (CFD) has proven itself a powerful tool in atmospheric modelling. By solving the Navier-Stokes equations and with correct description of the atmospheric boundary layer and turbulence at the domain boundaries, the local influences of the shore topography and the obstacles on the wind flows can be investigated in detail. Two examples of the use of CFD (Fluidyn PANWIND software) are presented here. The first one shows the coastal wind analysis of 2012 Olympic sailing site of Weymouth, UK. The local wind effects due to the harbour and hill have been determined and compared to observations of wind velocity and direction for several wind conditions. The second example required to model the wind over the training base of the French Sailing Team in Brest, France. This landlocked bay, surrounded by two steep hills and linked to the Atlantic Ocean by a strait, emphasizes the need for a CFD simulation of the wind which provided the patterns of wind around the racing area compared with empirical observations.

NOMENCLATURE

C_1	k - ϵ turbulence model constant
C_2	k - ϵ turbulence model constant
C_S	dimensionless turbulence production factor
C_E	dimensionless turbulence viscosity constant for the k - ϵ model
C_p	specific heat of air ($J g^{-1} K^{-1}$)
$F_{g/p}^*$	force due to: (g) gravitational acceleration, (p) interaction with droplets/particles ($N m^{-2}$)
g	gravitational acceleration ($9.8 m s^{-2}$)
G	turbulence production rate by shear = $\sigma \nabla u$ ($m^2 s^{-3}$)
h_m	specific enthalpy of species m ($J kg^{-1}$)
I	specific internal energy ($J kg^{-1}$)
J	heat flux vector ($W m^{-2}$)
k	turbulent kinetic energy per unit mass ($m^2 s^{-2}$)
k_c	thermal conductivity ($W m^{-1} K^{-1}$)
L	Monin-Obukhov turbulent length scale (m)
Q_h	rate of specific internal energy gain due to (h) surface energy budget ($J kg^{-1} s^{-1}$)
Ri	Richardson number, dimensionless
t	time since the start of the release (s)
T	temperature (K)
u	fluid velocity ($m s^{-1}$)
u^*	surface friction velocity ($m s^{-1}$)
v	wind speed ($m s^{-1}$)
W_p	Turbulence production due to interaction with particles ($m^2 s^{-3}$)
z	height (m)
z_0	ground roughness length (m)
Greek letters	
ρ	density of air
μ	primary (shear) viscosity of fluid ($kg m^{-1} s^{-1}$)
λ	secondary (bulk) viscosity of fluid ($kg m^{-1} s^{-1}$)
σ	Newtonian viscous stress tensor ($N m^{-2}$)
ϵ	dissipation of turbulent kinetic energy ($m^2 s^{-3}$)

ζ	Monin-Obukhov similarity variable = z/L , dimensionless
κ	Von Karman constant = 0.41, dimensionless
θ	potential temperature (K)
θ^*	temperature scale
σ_h	turbulent Prandtl number, dimensionless
σ_k	dimensionless turbulence model constant for the k equation
σ_ϵ	dimensionless turbulence model constant for the ϵ equation
$\Psi_{1/2}(\zeta)$	similarity profiles
ν_t	turbulent viscosity ($m^{-1} s^{-1}$)

1 INTRODUCTION

Accurate wind field description (wind speed, wind direction and turbulence) plays an important role for sailing competitions. The proper wind speed range for sailing is between 2.5-18 m/s. Traditional in-situ measurement data obtained are usually insufficient to characterise fully the flow, as data time series are too short, and only defined at a specific locations. Furthermore the interpolation wind flow models using mass consistent techniques which extrapolate the data from the point measurements (meteorological stations) do not provide the required accuracy over the entire area of interest.

The atmospheric circulation in the lower layers is particularly dependent on local effects due to complex terrain. The topography, the transition zones between land and sea (estuaries, bays,...), the different roughness surface (urban areas, forests...), contribute to modify large scale flows and these influences have to be evaluated in details.

The complex topography in coastal area emphasizes the need for a complete 3D CFD simulation of the wind. The wind flow modelling provides the patterns of wind speed and wind directions around the racing area.

In many wind studies, the objective is to analyse the sea breeze effect based on the statistics of synoptic and local weather station measurements. This paper mainly focuses on the local wind characteristics with a predefined wind boundary condition assumed constant and considering topographical and roughness effect. Two different interesting areas have been studied in the frame of this project.

Weymouth, a coastal city in Southern UK hosted the 2012 Olympic Sailing Events in August. The sailing competition spots are shown in Figure 1.

Weymouth is a city surrounded by sea and hills. In the south of the city, i.e., in the south-east of the sailing area, there is a hilly island named Portland (130m). The topography is complex and consequently the local wind flow can be very difficult to comprehend.

The second sailing area is located in the well-known roadstead (bay) of Brest, in Finistère department of France (see Figure 2). It is required to identify the characteristic of this water body into details to fully assess the impact of the surrounding topography. Indeed, it is a landlocked bay surrounded by two very steep hills (50 to 80 m) and linked to the Atlantic Ocean by a strait about 2 km wide with a 240° orientation.

The wind modelling focuses here on two main areas: the Queler Peninsula (2nd sub-domain) and the Cape of Armorique (3rd sub-domain)



Figure 1: Schematic map for sailing events in Weymouth



Figure 2: Area of interests in Brest roadstead

2 WIND FLOW MODELING

2.1 FLUIDYN-PANWIND

Fluidyn-PANWIND is a module of fluidyn-PANACHE family which allows a quick and accurate simulation of wind flows around buildings, hills at local or medium large scale by taking into account all kinds of obstacles, the topography, the influence of terrain and vegetation, the local meteorological conditions. The software solves the Navier-Stokes equations (Mass, energy and momentum conservation) with a finite volume method on structured or unstructured mesh.

In this code the mass conservation equation for total fluid density is expressed as

—

where ∇ is the gradient of the considered quantity.

The momentum conservation equation for the fluid mixture is

$$\frac{\partial \rho u}{\partial t} + \nabla \cdot [\rho u u + \sigma] = \nabla P + F_s + F_g + F_p$$

where σ is Newtonian viscous stress tensor ($\sigma = \mu[\nabla u + (\nabla u)^T] + \lambda(\nabla \cdot u)i, \mu, \lambda =$ first and second coefficients of viscosity, $\lambda = -2/3\mu$, $T =$ matrix transpose; $i =$ unit dyadic - product of vectors). The energy conservation equation is:

$$\frac{\partial \rho I}{\partial t} + \nabla \cdot [\rho u I + J] = \nabla \cdot \mathbf{u} + \rho \varepsilon + Q_h$$

Where I is the specific internal energy, J is the heat flux $= k_c \nabla T + \rho \sum [h_m \nabla(\rho_m/\rho)]$, Q_h is the rate of specific internal energy gain due surface energy budget.

2.2 GEOMETRY AND MESH

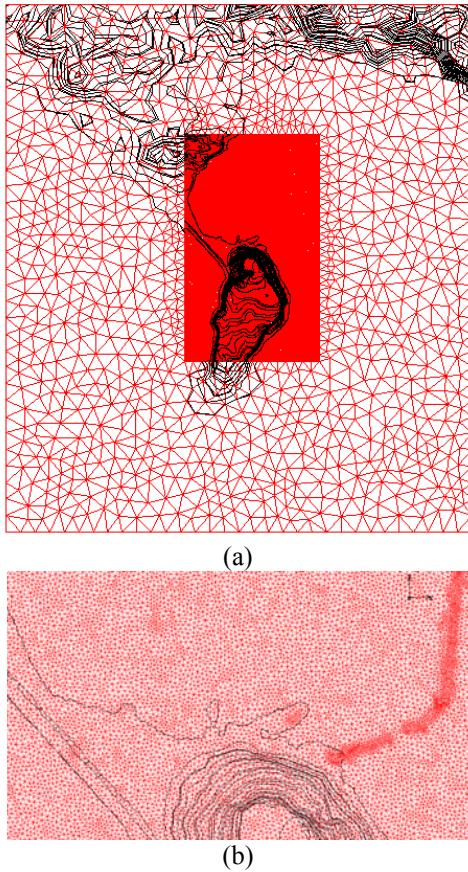


Figure 3: Weymouth unstructured mesh at ground level
(a) full domain (b) nested domain

For Weymouth case, the topography of the site was collected from Landform Profile Plus data on a global domain of 24 km * 25 km. This data has a 15–25 centimetre root mean square error (RMSE) accuracy and a grid resolution of 2 metres to 10 metres - sufficiently detailed to represent key terrain features. The harbour and jetties were modelled in finer details in an embedded domain of dimensions 5 km * 10 km. The finest cell size of the unstructured mesh in the harbour is 12 m and the averaged size dimension in

the sailing area is 25 m (see figure 3) resulting in a total of 2 million cells. Vertical mesh gets a 2m resolution from ground level to 12m of altitude. The vertical mesh is then coarser till until 200 m high.

A large main domain of 43km by 32km was used for Brest's Roadstead case. A first nested domain of 30 km*28 km has been defined. Two smaller embedded domains with an area around 80 km² were used in order to evaluate accurately the wind flows as shown in figure 2. The topography was extracted from The NASA Shuttle Radar Topographic Mission (SRTM) who has provided digital elevation data (DEMs) for over 80% of the globe. The SRTM data is available as 3 arc second (approx. 90m resolution) Digital Elevation Model.

The finest cell size of the unstructured mesh in the two nested domains is 30m and the averaged size dimension in the sailing area is 50m resulting in a 2.3 million cells. Vertical mesh gets a 3m resolution from ground level to 15m of altitude. The vertical mesh is then coarser until 200 m high.

2.3 TURBULENCE MODEL, BOUNDARY AND INITIAL CONDITIONS

The standard $k-\varepsilon$ model has been used throughout the simulations.

The $k-\varepsilon$ model is a two-equation linear eddy viscosity model. The PANACHE implementation of this model is derived from the standard high-Re form with corrections for buoyancy and compressibility. It solves the transport equations for turbulent kinetic energy, k , and its dissipation rate, ε . The incompressible versions of the equations are:

$$\frac{\partial k}{\partial t} + \nabla \cdot (\mathbf{U}k) = \nabla \cdot \left(\nu_t + \frac{\nu_t}{\sigma_k} \right) \nabla k + P_k + P_b - \varepsilon$$

$$\frac{\partial \varepsilon}{\partial t} + \nabla \cdot (\mathbf{U}\varepsilon) = \nabla \cdot \left(\nu_t + \frac{\nu_t}{\sigma_\varepsilon} \right) \nabla \varepsilon + \frac{\varepsilon}{k} [C_{\varepsilon 1} (P_k + C_b P_b) - C_{\varepsilon 2} \varepsilon]$$

where, $P_k = \nu_t \dot{\gamma} : \nabla \mathbf{U}$, the mechanical production rate

$$P_b = \nu_t \beta \frac{\mathbf{g} \cdot \nabla T}{\sigma_h}, \text{ the buoyancy production rate}$$

$\sigma_k =$ Prandtl number for turbulent diffusion of k

$\sigma_\varepsilon =$ Prandtl number for turbulent diffusion of ε

$\mu_t =$ turbulent eddy diffusivity

$C_{s1}, C_{s2} = k-\varepsilon$ turbulence model dimensionless constants

The eddy diffusivity is computed using:

$$\nu_t = C_E * \frac{k^2}{\varepsilon}$$

Ambient mean wind speed and air temperature profiles are specified within the model domain and are represented by logarithmic functions, such that:

$$v(z) = \frac{u^*}{\kappa} \left[\ln\left(\frac{z}{z_0}\right) \Psi_1(\zeta) \right]$$

$$\theta(z) = \sigma_h \frac{\theta^*}{\kappa} \left[\ln\left(\frac{z}{z_0}\right) \Psi_2(\zeta) \right]$$

Where θ^* = temperature scale; $\Psi_1(\zeta)$ and $\Psi_2(\zeta)$ = similarity profile.

The surface friction velocity, u^* , the temperature scale θ^* , and the Monin-Obukhov length, L are related by: $L = u^{*2} T / (g \kappa \theta^*)$ and $\theta^* = Q_h / (\rho C_p u^*)$.

The micrometeorological parameters u^* , θ^* , and L are evaluated for different atmospheric stability classes. They have been evaluated for neutral conditions.

In this study, the roughness length has been chosen equal to 0.001m (typical of water body). The roughness length for the land has been chosen equal to 0.4m.

2.4 SIMULATION AND SOLVER PARAMETERS

In the frame of this study, the solver is a pressure-based fully implicit segregated method on unstructured meshes. It is well suited for flows that are steady or quasi-unsteady (slowly changing).

It solves all governing equations separately. It uses an iterative procedure for both steady state and transient cases. SIMPLE scheme is used for pressure computation. It uses a formulation valid for flows at all speeds and for any thermodynamic model.

3 RESULTS

3.1 BREST ROADSTEAD CASE ANALYSIS

3.1.1. Climatology

The dominant flux in all seasons comes from west to west-southwest even if a few nuances exist depending on the season. The most significant factor is the south pathway of the low pressure zone. During winter, stronger west or southwest winds are usually observed and frequent disturbances which impact the Atlantic coast.

During the summer, this scheme remains relevant but strengthening anti-cyclonic depression requires a more northern flow, which allows the Atlantic coast to sample light winds and a more conventional summer time.

The North Atlantic Oscillation (NAO) is a climatic phenomenon in the North Atlantic Ocean of fluctuations in the difference of atmospheric pressure at sea level between the Icelandic low and the Azores high (see Figure 4). Through east-west oscillation motions of the Icelandic low and the Azores high, it controls the strength and direction of westerly winds across the North Atlantic.

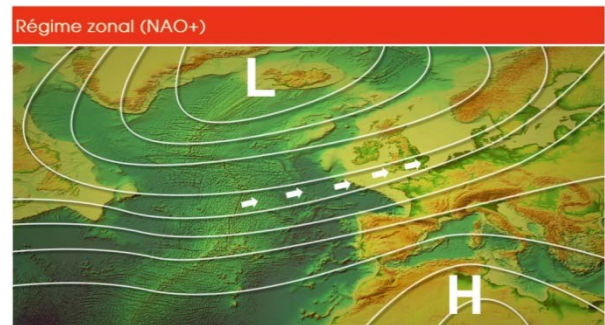


Figure 4: The North Atlantic Oscillation (NAO) is a climatic phenomenon in the North Atlantic Ocean - L : Low pressure area in Iceland - H: High pressure area in Azores and Northern Africa

3.1.2. Local effect of terrain on the wind flows

The results of the modelling focus on the wind direction modification due to the topography around the sailing area.

The wind directions are SW (225°) and E(90°) and the simulations were done for a wind speed of 10 m/s at a height of 10m for both directions.

In Figure 5, the white colour arrows and the pink colour contours represent a deviation greater than +15° from the mean direction and the black colour arrows and the blue colour contours indicate a deviation greater than -15°. All the views are voluntarily schematic for an easy understanding of the wind fields in the area by non-specialist people.

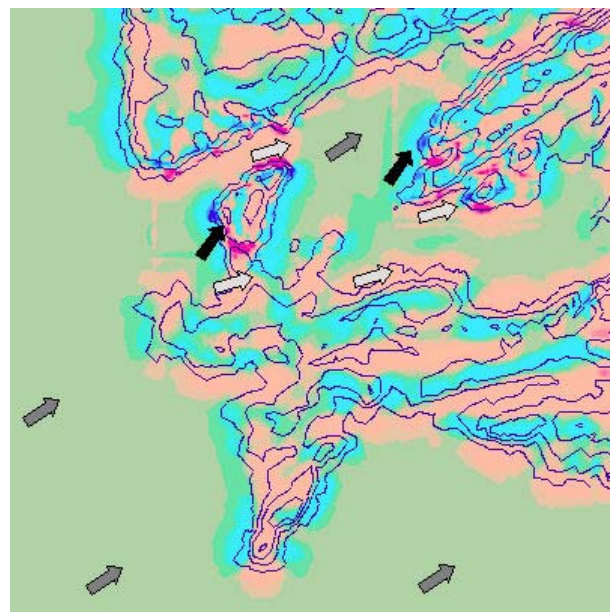


Figure 5: Wind deviation in case of SW conditions

The wind flow is channelled through the axis of the strait, except where a little deviation is observed near the tip of Spanish peninsula Quernel. The flow is divided in a West-Southwest and a South-Southwest part when reaching the peninsula of Plougastel (see figure 6).

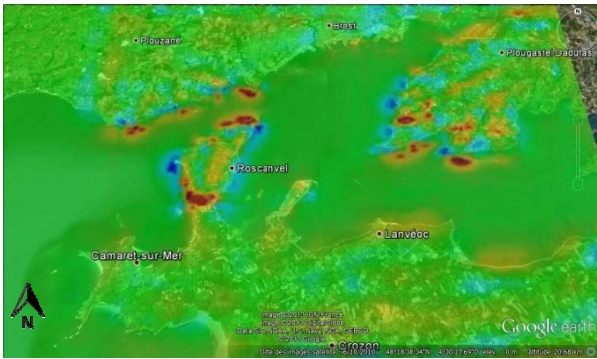


Figure 6: Wind direction contours for a wind condition 225° - 10 m/s (Google Earth view) – In blue color the negative deviation and in red color the positive deviation

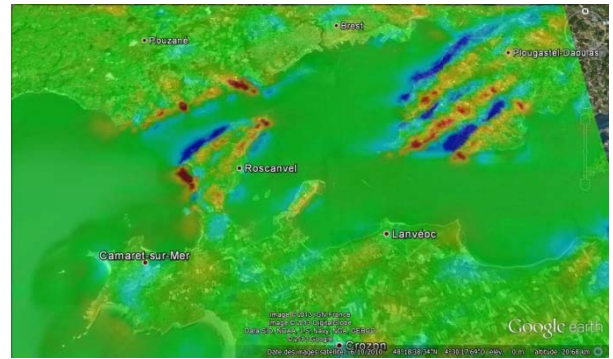


Figure 8: Wind direction contours for a wind condition 90° - 10 m/s on (Google Earth view) - In blue color the negative deviation and in red color the positive deviation

The results for the E condition (see Figures 7 and 8) show that the wind takes a North-East direction in the area between Brest and the peninsula of Plouganest. The effect of the tip of Armorique gives a southeast direction. In this area, the wind speed increases (see figure 9). In the strait, the wind takes a stable North-East direction. This is a classical phenomenon observed by the sailors in the area.

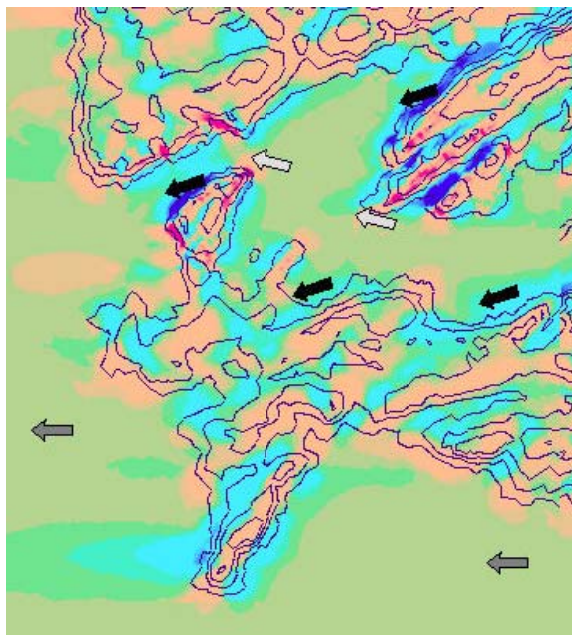


Figure 7: Wind deviation in case of E conditions

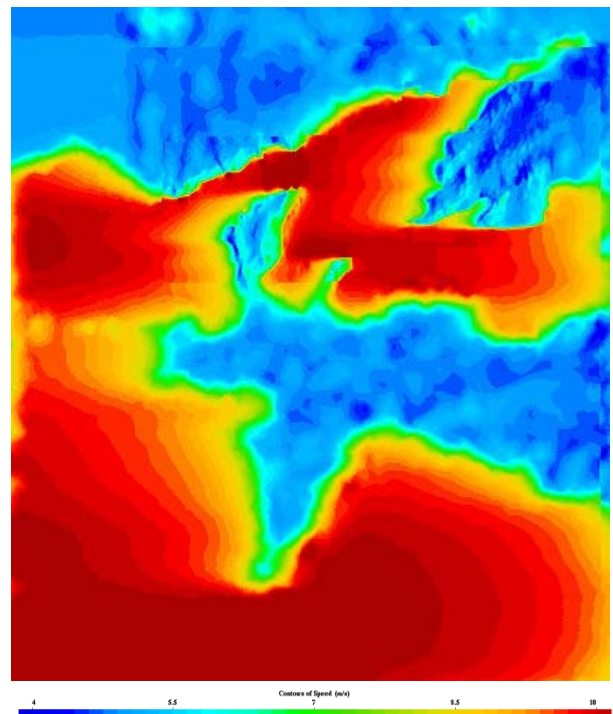


Figure 9: Wind speed contours at surface level for 90° - 10 m/s – In red colour, the wind speed is higher than 10 m/s and in blue color, the wind speed is lower than 4 m/s

3.2. WEYMOUTH CASE ANALYSIS

The results of the modelling focus on the wind direction modification due to the topography around the sailing area.

The wind directions are WSW (240° to 270°).

The wind keeps its initial direction (boundary conditions) in the middle of the harbour (zone 1 in figure 1) and in the middle of the bay (zone 6).

The wind velocity for the WSW direction remains high in most of the zone 1. Nevertheless, the velocity fields show low wind speed in the North of the zone 1 if the wind direction is more than 260°.

In the zone 2 (figure 1), there is a predominant influence of coastal landforms. The sailing in downwind area of hilly and disparate coast can be exposed to various effects within a few degrees of the wind direction.

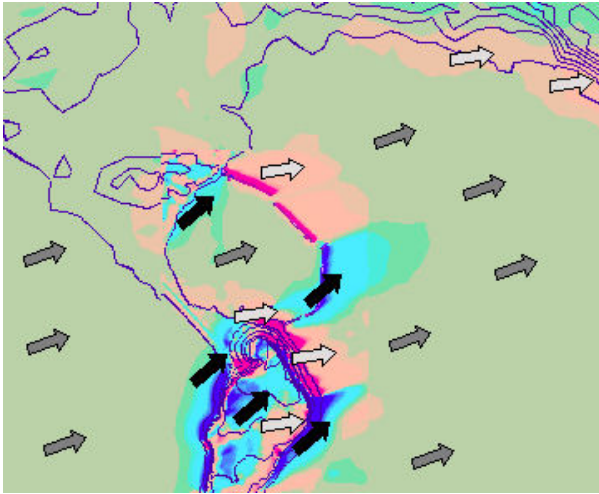


Figure 10: Wind deviation in case of WSW conditions

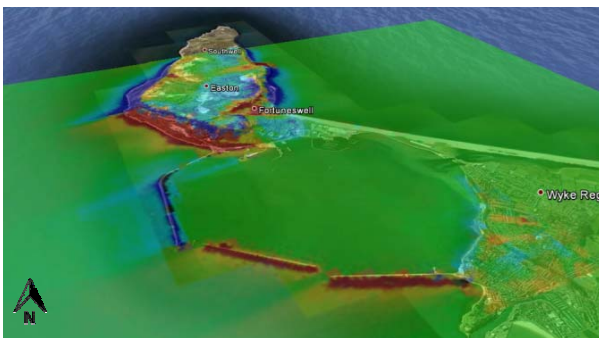


Figure 11: Wind direction or a260° - 10 m/s/wind condition (Google Earth view) - In blue color the negative deviation and in red color the positive deviation

6 CONCLUSIONS

In order to demonstrate the usefulness of CFD modelling for the purpose of wind predictions for sailing teams, two examples of the use of CFD through Fluidyn PANWIND dedicated software have been presented here. The first one shows the coastal wind analysis of 2012 Olympic sailing site of Weymouth, UK. The local wind effects due to the harbour and hill have been determined and compared to observations of wind velocity and direction for several wind conditions. The second example modelled the wind over the training base of the French Sailing Team in Brest, France. This landlocked bay surrounded by two steep hills and linked to the Atlantic Ocean by a strait. This simulation emphasized the need for a CFD simulation of the wind. This simulation provided the patterns of wind around

the racing area which are compared with empirical observations.

Although no quantitative results were yet available on these two sites, the qualitative assessment show a good agreement between the numerically predicted wind flows and the sailing team experience on the water. Further investigations will be carried out in order to compare measurements of the wind speed and direction.

REFERENCES

1. GRYNINGS.-E., BATCHVAROVAE., BRUMMERB., JØRGENSEN H., and LARSEN S., 'On the extension of the wind profile over homogeneous terrain beyond the surface layer', *Boundary-Layer Meteorol.*, **124**, pp251–268, 2007.
2. PEÑA A., 'Sensing the wind profile', Ph.D. Thesis, University of Copenhagen, March 2009.
3. PEÑA A., GRYNINGS.-E., 'Extending the wind profile much higher than the surface layer', *European Wind Energy Conference and Exhibition (EWEC)*, Marseille, France 16 - 19 March 2009.
4. BURCHARDH., 'Applied Turbulence Modelling in marine Waters', Springer, 2002.
5. BAUMERTH. Z. and PETERS H., 'Second-moment closures and length scales for weakly stratified turbulent shear flows', *J. Geophys. Res.*, **105** (C3), pp 6453-6468, 2000.
6. HAN J., ARYA S.P., SHEN S., and LIN Y-L.: An 'Estimation of Turbulent Kinetic Energy and Energy Dissipation Rate Based on Atmospheric Boundary Layer Similarity Theory', NASA/CR-2000-210298, June 2000.
7. PETERSH. and BAUMERTH. Z., 'Validating a turbulence closure against estuarine microstructure measurements', *Ocean Modelling*, **19**, pp183–203, 2007.
8. DUYNKERKE P.G., 'Application of the k-ε turbulence closure model to the neutral and stable atmospheric boundary layer', *J. Atmos. Sci.*, **45**(5), pp865-880, 1988.

AUTHORS BIOGRAPHY

M. Le Guellec holds the current position of Project Engineer at FLUIDYN FRANCE. He is responsible for environment impact studies and consequence assessment studies. His previous experience includes the wind field modelling at local scale in complex urban district for pedestrian comfort assessment and wind energy assessment in hilly region.

Y. Amice holds the current position of Chief Petty Weather, seconded by the Navy with the French Sailing Federation.